Wake Shapes Behind Wings in Close Formation Flight Near the Ground

Cheolheui Han
Kyungwon Tech, Yatap-Dong, Bundang-Gu, KyungKi-Do 463-827, Korea
Leesang Cho, Jinsoo Cho*
Department Mechaincal Engineering, Hanyang University, Seoul 133-791, Korea

The unsteady evolution of trailing vortex sheets behind wings in close formation flight near the ground is simulated using a discrete vortex method The ground effect is included by an image method The method is validated by comparing computed results with other numerical results. For a lifting line with an elliptic loading, the ground has an effect of moving wingtip vortices laterally outward and suppressing the development of vortex evolution The gap between wings in close formation flight has an effect of moving up wingtip vortices facing each other For wings flying in parallel, the ground effect causes the wingtip vortices facing each other to move up, and it makes the opposite wing tip vortices to move laterally outward When there is a relative height between the wings in ground effect, right-hand side wingtip vortices from a mothership move laterally inward.

Key Words : Formation Flight, Ground Effect, Aircraft Wake Vortices, Discrete Vortex Method

Nomenclature

b_H Nondimensionalized half-span of the hitchhiker aircraft by the half-span of the hitchhiker aircraft, (1)
b_M Half-span of the mothership divided by the half-span of the hitchhiker aircraft
$C(\Gamma, t)$ Point on a lifting line in the complex plane
$C'(\Gamma^o, t)$ Point on an image lifting line in the complex plane
dt Time step
dy Distance between the mothership and the hitchhiker divided by the half-span of the hitchhiker aircraft
dz Relative height between the mothership and the hitchhiker divided by the half-span of the hitchhiker aircraft
h Ground height, distance from a mothership to the ground
N Number of point vortices
γ Distance between the position of a vortex core and a point in space
r_c Vortex core radius
r_{c0} Initial vortex core radius
R_e Vortex Reynolds number
r_{ij} Distance from the i^{th} point to the j^{th} point
t Elapsed time, sec
T Total elapsed time, sec
u Induced velocity in downstream direction
$(u, v)_j^{Mm}$ Induced velocity at a wake vortex j on the mothership aircraft from other vortices on the image mothership aircraft
$(u, v)_j^{Mh}$ Induced velocity at a wake vortex j on the mothership aircraft by vortices on the image hitchhiker aircraft
$(u, v)_j^{Hm}$ Induced velocity at a wake vortex j on the hitchhiker aircraft by vortices from the

* Corresponding Author,
E-mail jscho@hanyang.ac.kr
TEL +82-2-2290-0429, **FAX** +82-2-2298-4634
Department Mechaincal Engineering, Hanyang University, Seoul 133-791, Korea (Manuscript **Received** August 20, 2004, **Revised** December 31, 2004)

image mothership aircraft

$(u, v)_j^{Hh}$ Induced velocity at a wake vortex j on the hitchhiker aircraft by other vortices on the image hitchhiker aircraft

$(u, v)_j^{MM}$ Induced velocity at a wake vortex j on the mothership aircraft from other vortices on the mothership aircraft

$(u, v)_j^{MH}$ Induced velocity at a wake vortex j on the mothership aircraft by vortices on the hitchhiker aircraft

$(u, v)_j^{HM}$ Induced velocity at a wake vortex j on the hitchhiker aircraft by vortices from the mothership aircraft

$(u, v)_j^{HH}$ Induced velocity at a wake vortex j on the hitchhiker aircraft by other vortices on the hitchhiker aircraft

v Induced velocity in spanwise direction

w Induced velocity in vertical direction

W Complex velocity potential

x Downstreamwise distance from a wing's trailing edge

y Spanwise distance from a wing's mid section

z Distance in vertical direction

$\bar{z}$ Complex conjugate of z in the complex plane

Greek

δ Smoothing factor

δt Time step

γ Vortex sheet strength

Γ Circulation of a lifting line at the point where the induced velocity is calculated

Γ_j Circulation of a vortex at the j^{th} point

Γ^* Circulation of a constant strength vortex sheet element on a lifting line

Γ_0 Maximum circulation

Γ_0^M Maximum circulation on the mothership for an elliptic load distribution

Γ_0^H Maximum circulation on the hitchhiker for an elliptic load distribution

Δt_g Growth age

τ Pseudo time

Abbreviations

AOA Angle of Attack

AR Aspect Ratio

IGE In Ground Effect

OGE Out of Ground Effect

1. Introduction

Recently, there has been great interest in engineering research inspired by mimicking nature (referred to as biommetics) The behavior of migratory birds has led to the study on achieving similar enhanced performance from multiple aircraft flying in formation Many military missions involve formation flight (Magill et al, 2003) Its primary purpose is for defense during its entire flight However, today's situations require reduction in fuel consumption in order to increase range and to reduce operational costs The important challenge in the study of formation flight is how to evaluate the aerodynamic interference between the aircraft in the formation While the increase in lift and drag reduction enhances the aerodynamic performance, additional yawing and rolling moments induce asymmetrical aerodynamic characteristics Compound Aircraft Transport (CAT) flight involves wingtip-docked or close-formation flight to utilize the mutual aerodynamic interaction benefits Wingtip-docked flight has the effect of increasing the total span of the aircraft system (Magill et al, 2003)

Most of the research in this area has been focused on analytical modeling based on potential flow theory Very few experimental data are shown in the published literature Blake (2000) used a Vortex-Lattice Method (VLM) to calculate the aerodynamic characteristics of a large number of vehicles in close formation flight He assumed that the wakes behind the aircraft were flat and parallel to the velocity vector of the aircraft. Wake-induced effects were investigated by changing lateral and vertical positions of the mothership and the hitchhiker Blake and Gingras (2001) performed a wind tunnel test of two delta wings flying in close proximity They also calculated the aerodynamic characteristics of those wings using the VLM They showed that the discrepancy between the measured data and the predicted results were mainly due to the incorrect representation of the wake shapes behind wings in close formation flight

Frazier and Gopalarathnam (2003) determined the optimal downwash distribution in the Trefftz plane using the calculus-of-variation approach of Jones (1950). The VLM is used to determine the optimum lift distributions while satisfying the constraints on the desired lift and desired zero rolling moment on each wing. Venkataramanan et al. (2003) developed a new technique for the trailing vortex effect modeling and incorporated it in a six-degree of freedom analysis of close formation. They included the effect of wake vortex decay in the model. The different geometrical dimension between the mothership and the hitchhiker was also included. Many of these investigations assumed a flat wake shape.

In most of the published literature, not much has been known on the wake roll-up behavior behind wings in close formation flight near the ground. Recently, Wang and Mook (2003) calculated the aerodynamic characteristics of formation flight of two rectangular wings using an unsteady vortex-lattice method. The calculated wake shapes represent a possible wake-wake interaction in close formation flight. Han and Cho (2004a) developed a discrete vortex method (DVM) that can be used for the simulation of wingtip vortices behind an elliptic loading or a fuselage/flap-wing configuration. Han and Cho (2004b) extended the method to the case of wings in close formation flight.

In this paper, the unsteady wake vortex evolution is investigated for wings in close formation flight near the ground. The discrete vortex method developed by Han and Cho (2004a and 2004b) is extended to the case of formation flight systems in ground effect. Load distributions along the lifting wings in formation flight are represented with point vortices with finite circulation. The trailing wakes from each wing are simulated by using the point vortices that deform freely with the assumption of a force-free position.

2. Discrete Vortex Method

The roll-up of a wake behind a finite span wing is a three-dimensional phenomenon. For a high aspect ratio (AR>3) wing that is at sufficiently low incidences (A.O.A.<5 degrees), the unsteady evolution of the wake vortices from the trailing edge is similar to the time-dependent self-induced deformation of an infinitely long vortex sheet. The vortex-sheet approach that is used here is appropriate at very high Reynolds numbers, since the wake vortices are then confined to a very thin region and the viscous effects are negligible outside of this region.

We follow the formulation of the roll-up of a vortex sheet as given by Birkhoff (1962). Consider a free vortex sheet which at time $t<0$ is stretched along the y-axis, the lines of constant vorticity are perpendicular to the (y, z) plane. The vortex sheet behind the lifting surface is represented as a curve $c(\Gamma, t)=y(\Gamma, t)+iz(\Gamma, t)$ in the complex plane. The circulation Γ is a Lagrangian parameter along the curve. The evolution equation for the vortex sheet is

$$\frac{\partial \bar{z}}{\partial t}=\frac{dW}{dc} \tag{1}$$

where the left-hand side is the Lagrangian velocity of a sheet fluid particle and the right-hand side is the Eulerian complex velocity field. Equation (1) represents the convection of a fluid particle at the local fluid velocity. For a vortex sheet with finite width, the complex velocity at an arbitrary point on the sheet is

$$\frac{dW}{dc}=\frac{1}{2\pi i}\oint\frac{d\Gamma^*}{c(\Gamma, t)-c(\Gamma^*, t)} \tag{2}$$

This integro-differential equation yields the time dependent velocity. The vortex sheet is represented as a series of straight-line segments (Fig. 1). Each segment is assumed to have a constant-strength vortex. This constant-strength vortex element is replaced by a single vortex with the same vorticity. On each line segment, a point vortex is located at the 3/4 point. In the case of a lifting line with elliptic loading, the circulation of the trailing horseshoe vortices is

$$G(y)=\frac{d\Gamma(y)}{dy}dy=\Gamma_0 y\left(1-\left(\frac{2y}{b}\right)^2\right)^{-1/2}dy \tag{3}$$

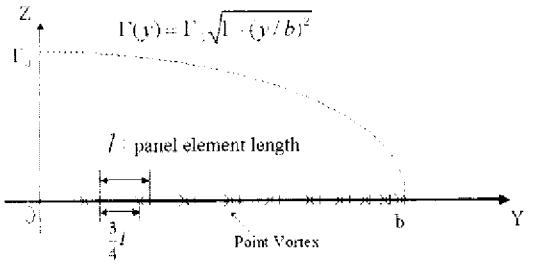

Fig. 1 Discrete vortex representation of a lifting line with elliptic loading

Since the complex number is a plane vector, the velocity components that are induced at the point (y_j, z_j) by a point vortex of strength G_i located at (y_i, z_i) is

$$v=\frac{G_i(z_j-z_i)}{2\pi r_{ji}^2},\quad w=-\frac{G_i(y_j-y_i)}{2\pi r_{ji}^2} \tag{4}$$

where r_{ji} is the distance from an i^{th} point where the point vortex is located, to the j^{th} point in space where the induced velocity is calculated.

The induced velocity at the point (y_j, z_j) from every vortex can be written as

$$\vec{w}_j=\frac{G_i}{2\pi}\sum_{i=1}^{N}\left(-\frac{(z_j-z_i)}{r_{ji}^2}\vec{i}-\frac{(y_j-y_i)}{r_{ji}^2}\vec{j}\right) \tag{5}$$

However, a real vortex is not a concentrated singularity of infinite vorticity. Ling et al.(1986) proposed a model that is based on the solution for the actual velocity that is induced by a vortex in a viscous fluid. The core radius r_c is approximately equal to the radial distance of the point where the maximum velocity is induced. This is expressed

$$r_c=r_{c0}+3.17\sqrt{\frac{\Delta t}{R_e}} \tag{6}$$

The second term on the right-hand side of Eq. (6) provides an estimate for the growth in the core radius of the vortex. The vortex Reynolds number is related to the time scale over which the laminar diffusion processes in the vortex core region becomes turbulent (Majda and Bertozzi, 2002). In the present work, an infinite Reynolds number is assumed. The velocity within the core (v_θ) is

$$v_\theta=\frac{\Gamma}{2\pi r}\left\{1-\exp\left[-1.25643\left(\frac{r}{r_c}\right)^2\right]\right\} \tag{7}$$

Outside the core region, the induced velocity is assumed to be that of a free vortex of strength Γ. This vortex core model is strictly valid only for a single viscous vortex in an unbounded incompressible flow (Leishman, 2000). Vortex methods therefore use several smoothing schemes to remove the infinite energy that results from the point-vortex discretization of the equations. Krasny (1987) avoids the singularity in the induced velocity of a point vortex through a smoothing factor, δ. The Eq. (5) can then be written as follows

$$\vec{w}_j=\frac{G_i}{2\pi}\sum_{i=1}^{N}\left(\frac{(z_j-z_i)}{r_{ji}^2}\vec{i}-\frac{(y_j-y_i)}{r_{ji}^2}\vec{j}\right) \tag{8}$$

For a wing with an elliptic loading, the circulation distribution along the spanwise direction is as follows.

$$\Gamma(y)=(1-y^2)^{\frac{1}{2}},\ |y|<1,\ t=0 \tag{9}$$

Thus, the strength of the vortex sheet has algebraic singularities at $y=\pm 1$. On the horizontal axis $z=0$, the sheet's velocity becomes infinite as $y\to 1$ from above and as $y\to -1$ from below. It is commonly known that the two ends of the vortex sheet roll-up into counter-rotating spirals. The non-uniqueness of the solutions to this initial-value problem has not yet been rigorously proven. However, the rolling-up of the vortex sheet is known as the physically reasonable solution (Krasny, 1987).

To enforce the no penetration condition at the ground, an image method is used. Since the wake is force-free, the evolution of each vortex is investigated by tracing the point vortices in pseudo-time τ and by moving the wake at the local flow velocity. The local flow velocity is the aggregate of the velocity components induced by all the vortices. To determine the roll-up of the wake at each time, the induced velocity $(u, v)_j$ at each vortex wake point j is calculated, and then the vortex elements are moved using an Euler convection scheme.

For a point vortex in the mothership,

$$(\Delta y, \Delta z)_j^M=[(v, w)_j^{MM}+(v, w)_j^{MH}]\,dt+[(v, w)_j^{Mm}+(v, w)_j^{Mh}]\,dt \tag{10}$$

And, for a point vortex in the hitchhiker,

$$(\Delta y, \Delta z)_j^H = [(v, w)_j^{HM} + (v, w)_j^{HH}]dt + [(v, w)_j^{Hm} + (v, w)_j^{Hh}]dt \quad (11)$$

There are three different regions in the aircraft wake. In the near field (several wing chords), the wake vortices are generated and the boundary layer is wrapped around the concentrated vortical structures. In the extended near field (several wing spans), the wake roll-up is completed. The merger process takes place, and the dynamics are essentially convective and weakly unsteady. In the far field, a single counter-rotating vortex pair begins to be influenced by the external turbulence, and vortex decay mechanisms starts (Majda and Bertozzi, 2002). The present method is an inviscid method, and the vortex merging or vortex decay is not applied to the present calculation. Thus, in this paper, inviscid wake shapes in the near and extended near field wake will be addressed.

3 Results and Discussion

The nomenclature for two wings in formation flight is shown in Fig. 2. The leading aircraft is called a mothership, and the following one is a hitchhiker. In this paper, only the case of close formation flight between the mother ship and the hitchhiker is investigated.

Modeling the wake behind a complex configuration is important because of the possible ill effects of the wake on the control surfaces. Figure 3 shows the simulated wake roll-up behavior for a fuselage and part-span flap configuration out of ground effect. In Fig.3, the present method is validated by comparing wake shape behind a lifting line with an elliptic loading with the published result of Krasny (1987). The smoothing factor has an effect of filtering the grid-scale noise and its choice for numerical simulation is usually based on machine precision. In this case, the smoothing factor is set to 0.05 [the same as Krasny's]. It can be deduced from Fig. 3 that the present results are in good agreement with Krasny (1987).

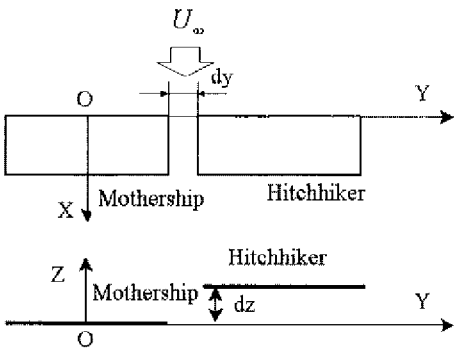

Fig. 2 Nomenclature for wings in close formation flight

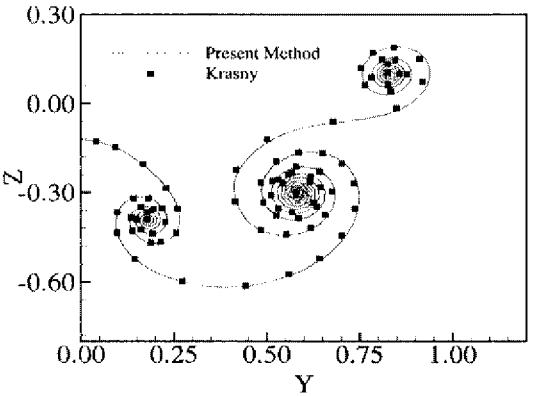

Fig. 3 Comparison of the present method to the result of Krasny (1987)

In Fig. 4, the ground effect on the unsteady evolution of the wake vortices is shown for a lifting line with elliptic loading. In the figure, the ground is when $z=0$. As the lifting line moves closer to the ground, the wingtip vortex has a reduced core size with its position moving laterally more outward. Because the desingularized point vortices are confined and coalesced into a small region, the total circulation decreases as the vortices evolve.

Figure 5 shows the movement of wingtip vortices when both the mothership and hitchhiker aircraft are flying close to each other. Their circulation strengths and spans are assumed to be equal. As the two wings are moving close to each other (dy=0.2, 0.5, 1.0), the wingtip vortices generated at the wingtips facing each other move up. The two opposite wingtip vortices maintain their positions essentially unaffected by the other aircraft. It is well known that the positions of

wingtip vortices behind aircraft are the function of wing loading, distance between vortices, and environmental factor such as turbulence. If the wing loadings of aircrafts are equal and the effect of environment is neglected, then the positions of vortices from those wings are the function of distance between the aircraft.

Figure 6 again shows the movement of wingtip vortices when both mothership and hitchhiker aircraft are in ground effect. In this case, the wingtip vortices generated at the wingtips facing each other moves more upward while the two opposite wingtip vortices maintain their positions unaffected by the other aircraft.

Figure 7 shows the ground effect on the wake shapes behind both the mothership and the hitchhiker. The ground height (h) is defined as a

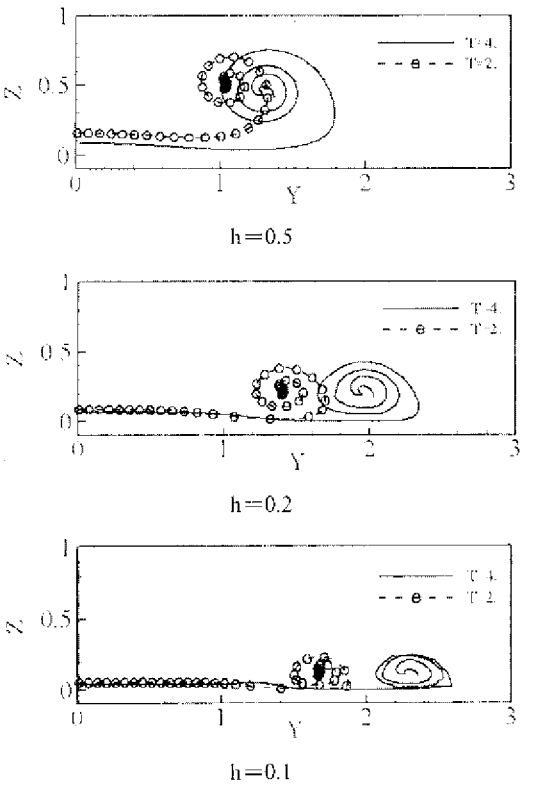

Fig. 4 Ground effect on the unsteady evolution of the vortex sheets (N=200, δt=0.01)

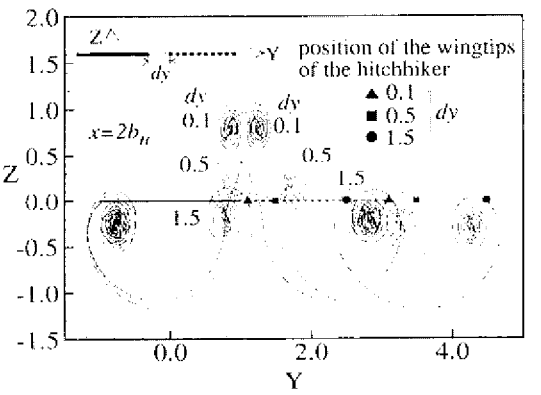

Fig. 5 Effect of gap on the positions of the wingtip vortices behind elliptically loaded wings in close formation flight, when two wings have the same wing loadings ($\Gamma_0^M=\Gamma_0^H=1.0$, $b_M=1.0$, $dz=0.0$, $dt=0.01$, $N=400$, OGE)

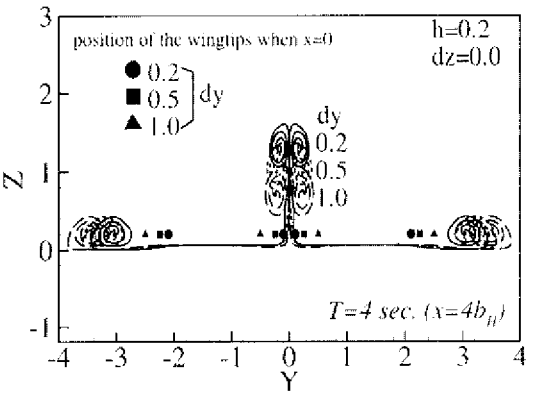

Fig. 6 Effect of gap on the positions of the wingtip vortices behind elliptic wings in close formation flight ($\Gamma_0^M=\Gamma_0^H=1$. and $b_M=b_H=2.0$, $dz=0.0$, $dt=0.01$, $N=400$, IGE)

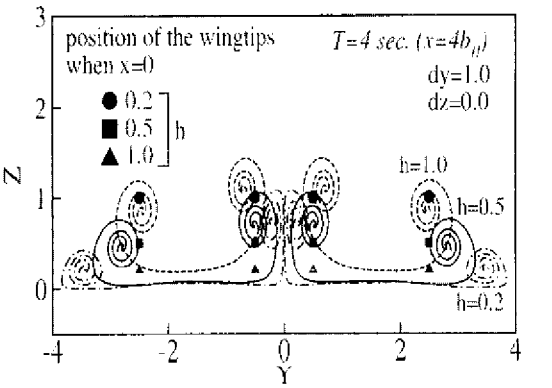

Fig. 7 Ground effect on the positions of the wingtip vortices behind elliptic wings in close formation flight ($\Gamma_0^M=\Gamma_0^H=1$. and $b_M=b_H=2.0$, $dz=0.0$, $dt=0.01$, $N=400$)

distance from a mothership to the ground. For a fixed value of gap (dy=1.0) and relative height (dz=0.0), the ground effect has an effect of both moving those wingtip vortices facing each other upward and two opposite wingtip vortices laterally outward.

Figures 8 and 9 show the ground effect on the wake shapes behind both the mothership and the hitchhiker. When there is the ground effect, the evolution of wingtip vortices is limited by the ground. Thus, the wingtip vortices are moving out laterally (See Fig.4). When the relative height between the wings is small, the vortices from a wing induce the upward velocities to the wingtip vortices from the other wing. The magnitude of the induced velocity is proportional to $1/r$. The wingtip vortices facing each other induce larger velocities than the two opposite wingtip vortices (See Fig.5). It can be deduced from Fig.8 and Fig. 9 that the position of wingtip vortices from the wings in formation flight near the ground is a function of both the relative distance between the wings and the ground height. Figure 9(a) shows the ground effect on the change of the position of wingtip vortices behind the mothership. The wingtip vortices from a wing both in and out of ground effect move upward in the vertical direction. However, the wingtip vortices from a wing in ground effect move laterally inward whereas those from a wing out of ground effect move outward. Figure 9(b) also shows the ground effect on the change of the position of wingtip vortices behind the hitchhiker. In this case, both wingtip vortices from the left-hand side of those

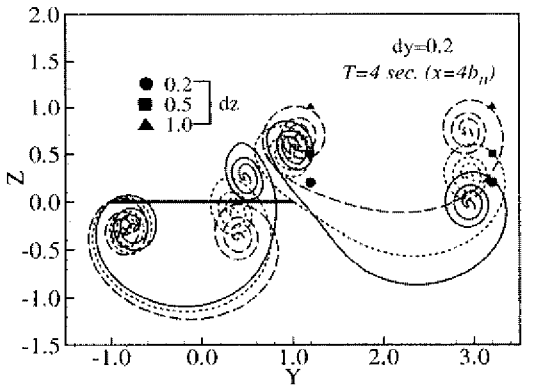

(a) OGE (h=∞)

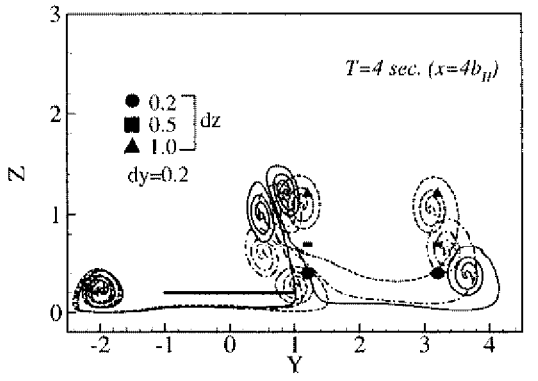

(b) IGE (h=0.2)

Fig. 8 Ground effect on the positions of the wingtip vortices when the relative height between the wings in close formation flight is changed ($\Gamma_0^M=\Gamma_0^H=1$, and $b_M=b_H=2.0$, $dy=0.2$, $dt=0.01$, $N=400$)

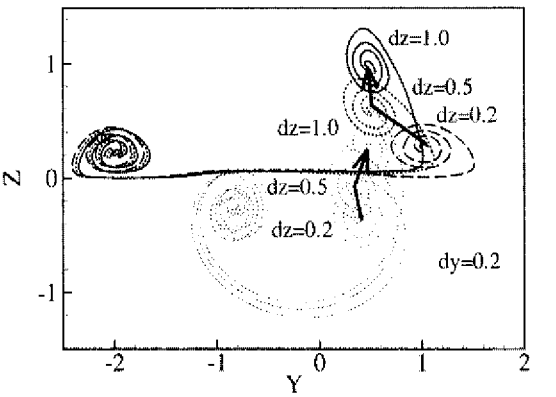

(a) Mothership

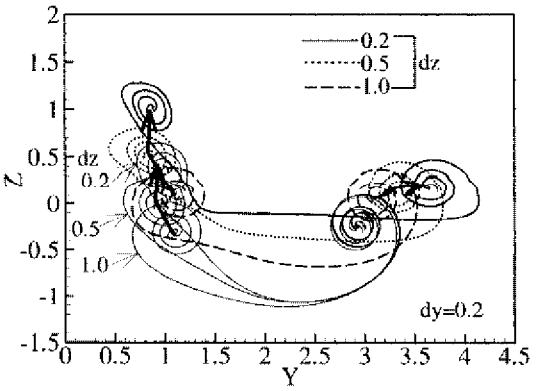

(b) Hitchhiker

Fig. 9 Reproduced figures from Fig. 8 to show wingtip vortex movements of the mothership and the hitchhiker, respectively

wings in and out of ground effect move upward in the vertical direction and outward in the lateral direction The wingtip vortices from the right-hand side of the wing in ground effect move laterally outward, whereas those vortices from the right-hand side of the wing out of ground effect remain unaffected from other wingtip vortices.

5. Conclusions

A study of the wake shape behind wings in close formation near the ground was done using a discrete vortex method The gap between the wings has an effect of moving up the wake vortices behind wingtips facing each other. For the wings flying in parallel, the ground effect causes the wingtip vortices facing each other to move up, and it makes the opposite wing tip vortices to move laterally outward When there is a relative height between the wings in ground effect, the right-hand side wingtip vortices from the mothership move laterally inward

Acknowledgment

This work was also supported by the Post-doctoral Fellowship Program of Korea Science & Engineering Foundation (KOSEF)

References

Betz, A , 1935, *Aerodynamic Theory*, Vol IV, Edited by Durand, W F , California Institute of Technology, pp 63~72

Birkhoff, G., 1962, "Helmholz and Taylor Instability," *Proc Symp Appl. Math Am. Math Soc* , Vol 8

Blake, W. B , 2000, "An Aerodynamic Model for Simulations of Close Formation Flight," *AIAA Modeling and Simulation Technologies Conference and Exhibit*, Denver, CO, AIAA -2000-4304, August 14-17

Blake, W B and Gingras, D. R , 2001, "Comparison of Predicted and Measured Formation Flight Interference Effects," *AIAA Atmospheric Flight Mechanics Conference and Exhibit*, Montreal Canada, AIAA 2001-4136, August 6-9

Frazier, J W and Gopalarathnam, A , 2003, "Optimum Downwash Behind Wings in Formation Flight," *AIAA Journal of Aircraft*, Vol 40, No 4, pp 799~803

Han, C and Cho, J , 2004, "Unsteady Trailing Vortex Evolution Behind a Wing In Ground Effect," *AIAA Journal of Aircraft* (In Print)

Han, C and Mason, W H , 2004, "Wingtip Vortex Behavior Behind Unmanned Aerial Vehicles in Close Formation Flight," *AIAA Journal of Aircraft* (In Print)

Jones, R. T , 1950, "The Spanwise Distribution of Lift for Minimum Induced Drag for Wings Having a Given Lift and a Given Bending Moment," *NACA TN* 2249

Krasny, R , 1987, "Computation of Vortex Sheet Roll-up In the Trefftz Plane," *Journal of Fluid Mechanics*, Vol 184, pp 123~155

Leishman, J G , 2000, *Principles of Helicopter Aerodynamics*, Cambridge University Press, pp 435~443

Ling, G C , Bearman, P W and Graham, J M R , 1986, "A Further Simulation of Starting Flow around a Flat Plate by a Discrete Vortex Model," *Internal Seminar on Engineering Applications of the Surface and Cloud Vorticity Methods*, Vol 51, No 14, Wroclaw, Poland, pp 118~138

Majda, A J and Bertozzi, A L , 2002, *Vorticity and Incompressible Flow*, Cambridge University Press, pp 359~382

Magill, S A , Schetz, J A and Mason, W H , 2003, "Compound Aircraft Transport A Comparison of Wingtip-Docked and Close-Formation Flight," *41st Aerospace Sciences Meeting and Exhibit, Reno*, Nevada, AIAA 2003-607, January 6-9

Venkataramanan, S , Dogan, A and Blake, W B , 2003, "Vortex Effect Modelling in Aircraft Formation Flight," *AIAA Atmospheric Flight Mechanics Conference and Exhibit*, Austin, TX, AIAA 2003-5385, August 11-14

Wang, Z. and Mook, D., 2003, "Numerical Aerodynamic Analysis of Formation Flight," *41st Aerospace Sciences Meeting and Exhibit*, Reno, NV, AIAA Paper 2003-610